

# Optical Interconnection in Silicon LSI

Shin Yokoyama, Yuichiro Tanushi, and Masato Suzuki

Research Center for Nanodevices and Systems, Hiroshima University

1-4-2 Kagamiyama, Higashi-Hiroshima, 739-8527, Japan

Phone: +81-82-424-6266, Fax: +81-82-424-3499, E-mail: yokoyama@xsxsys.hiroshima-u.ac.jp

## 1. Introduction

Recently, the research field called "Silicon Photonics," in which the silicon based photonic devices are integrated in silicon LSI, is attracting great attention in order to overcome the problem of signal delay in the global metal interconnection in the LSI [1-5]. We have been studying optical interconnection in LSI from twenty years ago [6]. The final target is to realize the optically interconnected LSI as shown in Fig. 1 [7]. In the 21st century center of excellence (COE) program, the research objective is to study the compact ring-resonator optical switches using electro-optic (EO) and magneto-optic (MO) materials or Si, which can be monolithically integrated in Si LSI especially on the metallization layer at low temperatures below 450°C (Fig. 1).

## 2. Ring resonator optical switches using electro-optic material

The structure of the ring resonator optical switch using EO material is shown in the inset of Fig. 1. When the optical path length of the ring equals to the wavelength times integer, the resonance occurs and the output light intensity has a peak, i.e.,

$$\lambda = \frac{2\pi R n_{eff}}{m} \quad (1)$$

Here,  $\lambda$  is the resonance wavelength,  $R$  is the ring radius and  $n_{eff}$  is the effective refractive index of the ring and  $m$  is an integer.

We have calculated the operation voltage of the ring resonator switch [8]. The right hand figure in Fig. 2 shows the structure used for the calculation. The vertical stack consisting of upper and bottom cladding layers, and middle core layer made of EO material, is used. The operation voltage is given by the following equations:

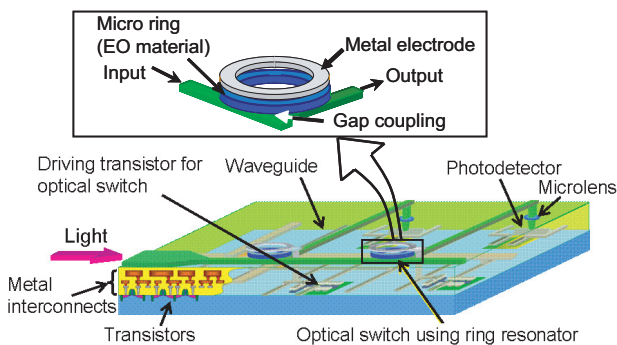


Fig. 1 LSI with optical interconnection, which operates at >10 GHz and is the target of this research.

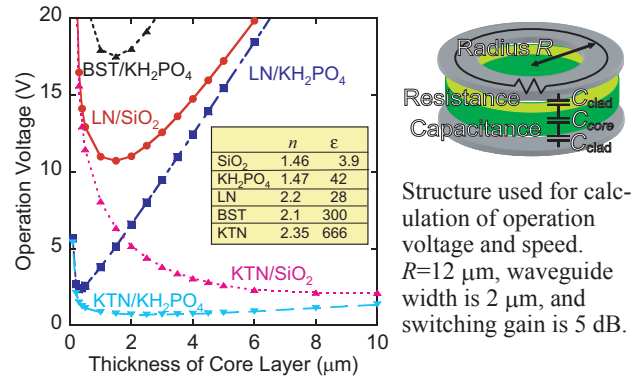


Fig. 2 Operation voltage versus core thickness of the ring resonator optical switches with various combinations of core and cladding materials.

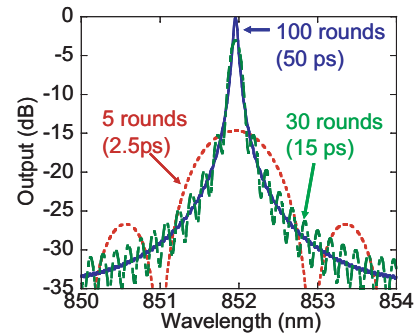


Fig. 3 Change in resonance characteristics with round time of the light in the ring. Coupling constant between I/O waveguide is 0.2, and bending loss is neglected.

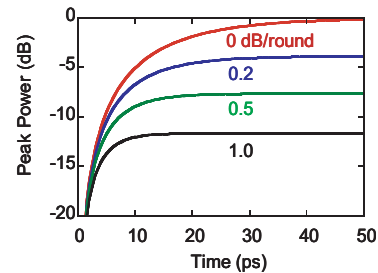


Fig. 4 Time dependence of peak power with a parameter of bending loss. High loss leads to quick saturation of the peak power but causes a broad peak.

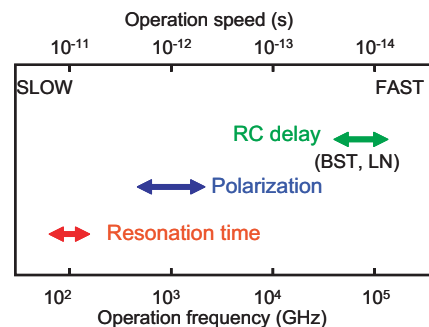


Fig. 5 Operation speed (or frequency) of ring resonator switch determined by various effects.

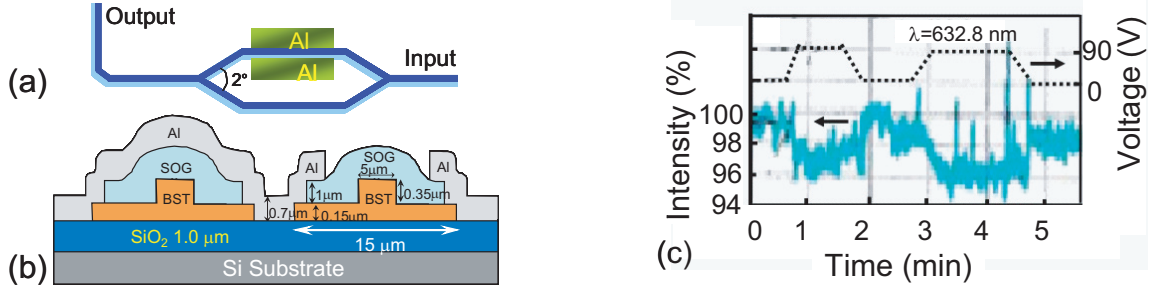


Fig. 6 (a) Schematic of Mach-Zehnder interferometer using electro-optic material (Ba,Sr)TiO<sub>3</sub> (BST), (b) cross section, and (c) modulation behavior of output light intensity by applied voltage. The BST film was formed by metal organic decomposition (MOD) method and annealed at 550°C for 2 h.

$$\left. \begin{aligned} \Delta n &= -\frac{1}{2} n_{eff}^3 r E, \\ V &= D_{core} E + 2 D_{clad} \frac{\epsilon_{core}}{\epsilon_{clad}} E. \end{aligned} \right\} \quad (2)$$

Here,  $\Delta n$  is the change in the refractive index due to the electric field  $E$ ,  $r$  is the electro-optic coefficient,  $D_{core}$  and  $D_{clad}$  are, respectively, thicknesses of the core and cladding layers,  $\epsilon_{core}$  and  $\epsilon_{clad}$  are, respectively, the dielectric constants of the core and cladding layers. Figure 2 shows the calculated operation voltage versus core thickness for various combinations of core and cladding materials. LN denotes LiNbO<sub>3</sub>, BST denotes (Ba,Sr)TiO<sub>3</sub>, and KTN denotes K(Ta,Nb)O<sub>3</sub>. The thickness of the cladding layer is chosen to obtain a light propagation loss less than 0.1 dB/cm and  $E$  is chosen to obtain a switching gain of 5 dB at wavelength of 852 nm. Ring radius and waveguide width are, respectively, 12 μm and 2 μm. For the combination of BST and KH<sub>2</sub>PO<sub>4</sub>, the minimum operation voltage becomes 17.5 V. For the combination of KTN/KH<sub>2</sub>PO<sub>4</sub>, it becomes 0.7 V.

Next, the switching speed is estimated [8]. Figure 3 shows the change in resonance characteristics with round time of the light in the ring. Coupling constant between input/output (I/O) waveguides is 0.2, and bending loss is neglected. With increasing the round time, the resonance peak becomes sharp. The peak intensity of the resonance curve is plotted as a function of round time in Fig. 4 with a parameter of the bending loss. The resonance time is roughly 15 ps and not strongly dependent on the bending loss. The other possible origins for the switching speed are  $RC$  delay and the polarization time of the EO material, which are compared in Fig. 5. The main cause which de-

termines the switching speed of the ring resonator switch is found to be a resonance time, and the operation frequency becomes >66 GHz which is faster than Si optical switch [2] by about one order of magnitude.

### 3. Mach-Zehnder modulator using EO material

We have employed (Ba,Sr)TiO<sub>3</sub> (BST) as EO material because it was already introduced in the Si LSI as a high dielectric insulator of the memory capacitor in the research stage [9]. Before fabrication of ring resonator, we have fabricated Mach-Zehnder interferometer (MZI) as shown in Fig. 6 in order to evaluate the optical property and electro-optic coefficient of the BST film. By using metal organic decomposition (MOD) BST films, we have, for the first time, succeeded in observation of the optical modulation in the BST MZI as shown in Fig. 6(c) [10]. The electro-optic coefficient calculated from the result in Fig. 6 is  $r=6.7$  pm/V which is about 1/5 of the single crystal LiNbO<sub>3</sub>. Although the modulation efficiency observed in this study is very small (~2%), it is meaningful that the optical modulation using monolithically integrated device on Si is achieved.

Next, we have studied the sputter deposited BST film. Figure 7 shows the structure of the fabricated MZI using BST film deposited by RF sputtering at 450°C. Because of the high optical loss, the BST waveguide is used only at the phase shifter of the MZI and the other part is made of silicon nitride. Figure 8 shows the relation between optical loss and crystallinity evaluated by the x-ray diffraction (XRD) (200) peak of the BST film deposited by RF sputtering. It is found that the high crystallinity results in the large optical loss, which may be caused by

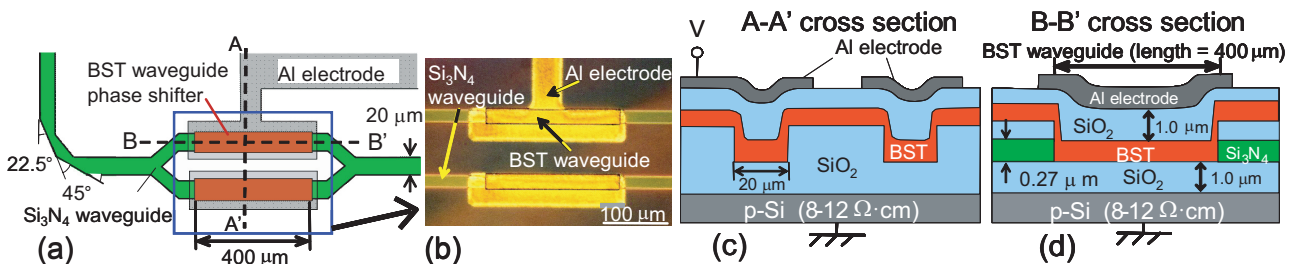


Fig. 7 (a) Schematic of hybrid Mach-Zehnder interferometer using sputtered (Ba,Sr)TiO<sub>3</sub> and silicon nitride films, (b) photograph of fabricated Mach-Zehnder interferometer, (c) cross section along A-A', and (d) cross section along B-B'. The BST film was formed by RF sputtering at 450°C.

the light scattering at the grain boundaries in the polycrystalline BST film. Figure 9 shows the light modulation characteristics of the MZI using BST film sputtered at 450°C, which is an acceptable process temperature after metallization. The modulation of ~10% is achieved at the electric field of  $1.2 \times 10^4$  V/cm. From this result, the electro-optic coefficient of 25.2 pm/V is estimated, which is comparable to that of single crystal LiNbO<sub>3</sub>. However, the response time is very long (1-6 s) as shown in Fig. 9, which may be due to the nonstoichiometry of the BST film [11, 12]. These disadvantages (low modulation efficiency and slow response) will be improved by improving the film quality and optimum device design.

#### 4. Optical switches using magneto-optic material

We have proposed a ring resonator optical switch using magneto-optic (MO) materials as shown in Fig. 10. The merit of this device is a low operation voltage less than 0.1 V. From the simulation we have found that the resonance peak splits to double peaks by applying the magnetic field (Fig. 11). The switching gain more than 10 dB can be obtained when Bi substituted Y<sub>3</sub>Fe<sub>5</sub>O<sub>12</sub> film is used [13]. The interesting finding is that the polarizer is not necessary although the conventional MO devices require the polarizer. We have deposited Bi<sub>3</sub>Fe<sub>5</sub>O<sub>12</sub> (BIG) film by RF sputtering at room temperature (amorphous film) and measured the Faraday effect using the measurement apparatus shown in Fig. 12. The result is shown in Fig. 13, which indicates the Faraday effect and the light modulation of ~2% is achieved [14].

#### 5. Optical switches using Si ring resonator

We are also studying the optical switches using Si ring resonator on SOI wafer (Fig. 14). Qianfan Xu *et al.* reported the plane type Si ring resonator switches operating at 1.5 Gb/s [4]. We proposed the stack type structure, in which the coupling efficiency between the ring and the I/O waveguides is more precisely controlled than the plane type ring resonators (Fig. 14). We have measured the optical modulation by the pumping light irradiation because the Al electrode is not completed yet. By irradiating the He-Ne laser light (633 nm), the electron-hole pairs are generated in the ring and the refractive index is changed, which leads to the change in the resonance wavelength. Figure 15 shows the modulation of the output light ( $\lambda=1299$  nm) intensity. When the resonance occurs, the output light intensity decreases because the light is absorbed by the ring. The measured data indicate that the resonance occurs by irradiating He-Ne laser and the output intensity decreases by ~3%.

#### 5. Integration of photodetectors

Integration of high-speed photodetectors is necessary to realize the LSI with optical interconnection. For the

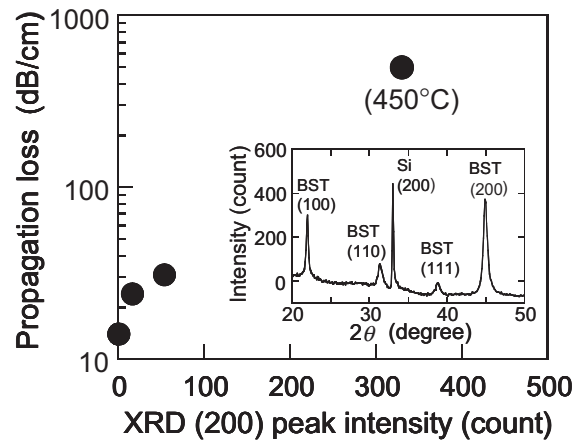


Fig. 8 Light propagation loss versus (200) x-ray diffraction (XRD) peak intensity of the sputtered BST film. High crystallinity causes the large propagation loss. Inset shows a typical XRD spectrum of the BST film deposited at 450°C.

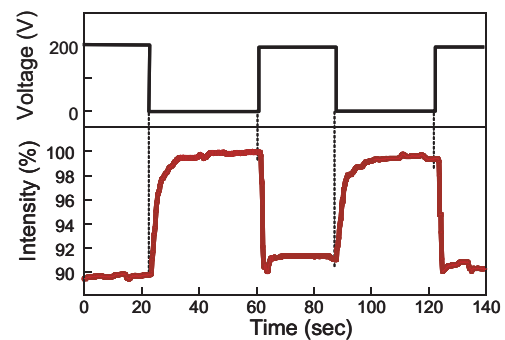


Fig. 9 Light modulation characteristics of the Mach-Zehnder interferometer using BST film sputtered at 450°C, which is an acceptable process temperature after metallization.

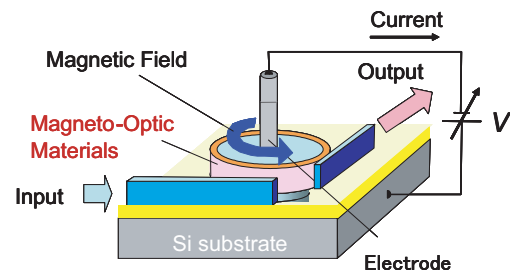


Fig. 10 Ring resonator optical switch using magneto-optic material.

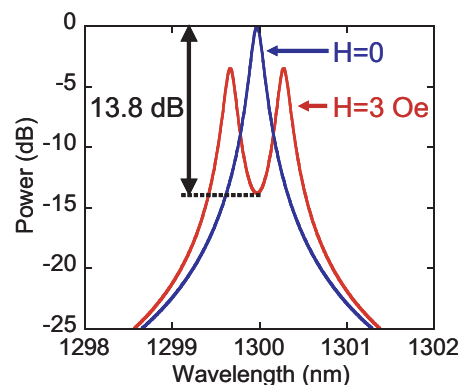


Fig. 11 Simulated resonance characteristics of the ring resonator using magneto-optic material (bismuth substituted Y<sub>3</sub>Fe<sub>5</sub>O<sub>12</sub>). Resonance peak splits to two peaks when magnetic field is applied.

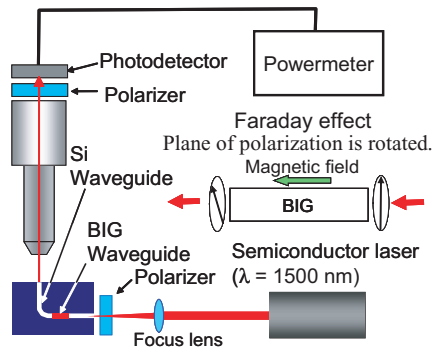


Fig. 12 Measurement apparatus for Faraday effect of  $\text{Bi}_3\text{Fe}_5\text{O}_{12}$  (BIG) waveguide.

EO material BST, the visible light can be used. Then Si photodetectors are available. On the other hand, for the MO material BIG or Si, the infrared light is necessary, then the SiGe photodetectors should be employed. We have designed and fabricated Si  $n^+p-p^+$  photodetectors as shown in Fig. 16(a) with cooperation with Prof. Miura in this COE group [15]. Although the simulated operation speed is in the order of 10 GHz, the fabricated device exhibited the slower speed of 300 MHz (Fig. 16(b)). The reason of the slow speed may be due to the degraded  $p^+/p$  or  $p/n^+$  junctions. We are now trying to clear the reason.

### Conclusions

We have, for the first time, demonstrated the light modulation by using the BST MZI monolithically integrated on Si substrate at  $450^\circ\text{C}$ . The result on MO optical modulator, stack type Si ring resonator switches, and integrated Si  $n^+p-p^+$  photodetectors are described.

### References

- [1] L. Pavesi and D. J. Lockwood ed, Topics in Applied Physics **94**: Silicon Photonics, Springer (2003).
- [2] A. Liu *et al.*, Nature **427**, 615 (2004).
- [3] H. Rong *et al.*, Nature **433**, 725 (2005).
- [4] Q. Xu *et al.*, Nature **435**, 325 (2005).
- [5] R. S. Jacobsen *et al.*, Nature **441**, 199 (2006).
- [6] M. Hirose *et al.*, Jpn. Patent Appl. No. 1846592 (1984).
- [7] M. Suzuki *et al.*, Jpn. J. Appl. Phys. **45**, No. 4B, 3488 (2006).
- [8] Y. Tanushi *et al.*, Jpn. J. Appl. Phys. **45**, No. 4B, 3493 (2006).
- [9] H. Yamaguchi *et al.*, Ext. Abst. IEEE IEDM (1996) p. 675.
- [10] Zhimou Xu *et al.*, Appl. Phys. Lett, **88**, No. 16, 161107 (2006).
- [11] M. Suzuki *et al.*, Ext. Abst. SSDM (2006) p. 48.
- [12] M. Suzuki *et al.*, to be published in Jpn. J. Appl. Phys. **46**, (2006).
- [13] Y. Tanushi *et al.*, 2nd Intern. Conf. on Group IV Photonics (Antwerp, Belgium, 2005) p. 165.
- [14] Y. Shishido *et al.*, to be presented at 2007 Spring JSAP Annual Meeting.
- [15] K. Konno *et al.*, J. Appl. Phys. **96**, 3839 (2004).

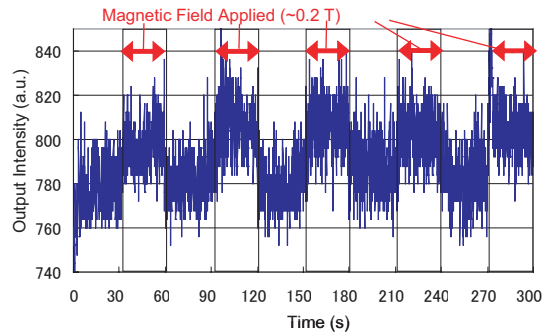


Fig. 13 Measured Faraday effect of BIG film sputtered at room temperature.  $\sim 2\%$  modulation is achieved at an external magnetic field of  $\sim 0.2$  T.

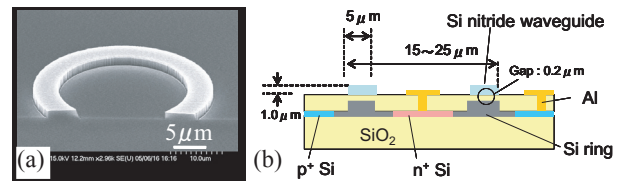


Fig. 14 (a) SEM photograph of fabricated silicon ring resonator on SOI wafer and (b) its cross section.

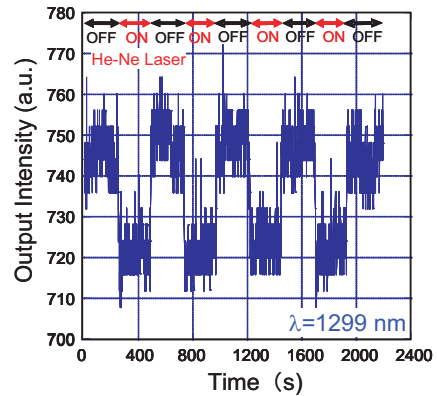


Fig. 15 Modulation of output light intensity by irradiation of He-Ne laser light.  $\sim 3\%$  modulation is achieved.

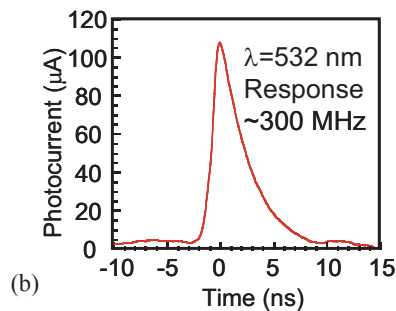
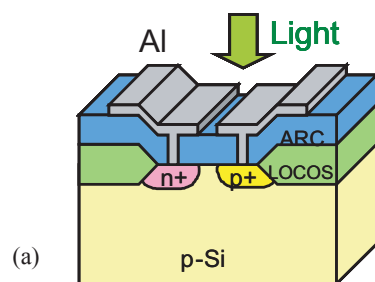


Fig. 16 (a)  $n^+p-p^+$  photodetector suitable for integration in silicon LSI and (b) its response for a 532 nm-pulse laser with pulse duration of  $\sim 1$  ns FWHM.